RSC Advances

ROYAL SOCIETY OF CHEMISTRY

www.rsc.org/advances

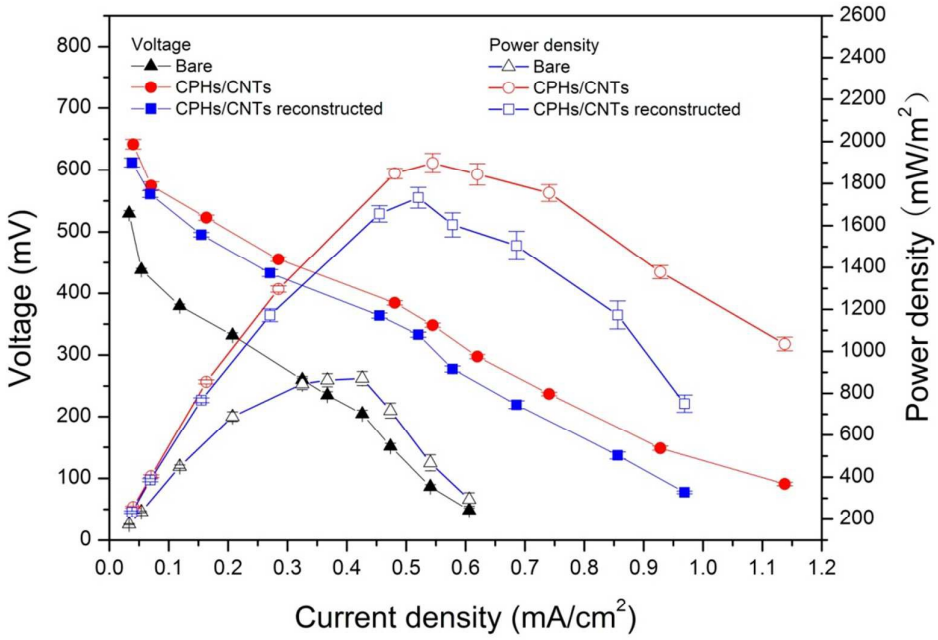

Polypyrrole hydrogels/carbon nanotubes enhanced electrocatalytic activity, biocompatibility and power density in microbial fuel cells.

Conductive polypyrrole hydrogels and carbon nanotubes composite as an anode for microbial fuel cells

Xinhua Tang[a,b], Haoran Li[c], Zhuwei Du[c], Weida Wang[d], How Yong Ng[a,*]

[a]National University of Singapore, Department of Civil and Environmental Engineering, Centre for Water Research, Singapore 117576, Singapore

[b]National University of Singapore, NUS Graduate School for Integrative Sciences and Engineering, Singapore 117456, Singapore

[c]Chinese Academy of Sciences, Institute of Process Engineering, National Key Laboratory of Biochemical Engineering, Beijing 100190, China

[d]University of Science and Technology Beijing, Civil and Environment Engineering School, Beijing 100083, China

ABSTRACT

Conducting polymer hydrogels, a unique class of materials having the advantageous features of both hydrogels and organic conductors, represent excellent electrochemical properties due to their intrinsic porous structure. Here, we reported a facile and scalable method to synthesize conductive polypyrrole hydrogels/carbon nanotubes (CPHs/CNTs) using phytic acid as gelator and dopant, and this composite was used as an anode in a dual-chamber microbial fuel cell (MFC). The high electrocatalytic activity of this material significantly reduced the interfacial charge transfer resistance and facilitated the extracellular electron transfer on anode surface. The three dimensional porous structure and hydrophilicity of this composite enhanced the biofilm formation on anode surface. CPHs/CNTs anode increased the maximum power density from 871 ± 33 mW/m^2 to 1898 ± 46 mW/m^2 and exhibited high stability

* Corresponding author. Tel.: +65 65164777; fax: +65 67744202.
E-mail address: howyongng@nus.edu.sg (H.Y. Ng)

in the two-chambered MFC. These results demonstrated that the synthesis of the CPHs/CNTs composite offered an effective approach to enhance the power production in MFCs.

Keywords: Microbial fuel cell; Power density; Conductive polymer hydrogels; Carbon nanotubes; Anode modification.

1. Introduction

Microbial fuel cell (MFC) is a bioelectrochemical system that converts chemical energy in organic matters into electrical energy by catalysis of microorganisms[1-2]. As a promising environmental biotechnology for wastewater treatment and renewable energy production, MFC has drawn much attention in the past decade[3-4]. Great progress has been made in this field and this technology has demonstrated its potential for applications such as wastewater treatment, biochemical oxygen demand detection, energy production, chemical and fuel synthesis and bioremediation[5-10]. However, the practical applications of MFCs are still limited due to the relatively small power density. The extracellular electron transfer from bacteria to electrode, a key parameter that defines the theoretical limits of energy conversion, is currently a limiting factor in enhancing the power density of MFCs[11-12]. Therefore, great efforts should be made to facilitate the extracellular electron transfer in order to boost the power generation of MFCs.

Anode material plays a key role in determining the power production of MFCs, because it not only influences the biofim formation on electrode surface, but also affects the extracellular electron transfer between microorganisms and the electrode. To date, carbon materials such as carbon paper, carbon cloth and graphite felt are the most commonly used anodes in MFCs due to their excellent biocompatibility, high specific surface area, high conductivity and strong stability in a microbial inoculum

mixture[13]. However, these carbon materials demonstrate very low electrocatalytic activity for the anode microbial reactions and the electron transfer efficiency needs to be improved[14]. As a result, development of anode material with high electrocatalytic activity and excellent biocompatibility is an effective approach to accelerate the electron transfer and enhance power production in MFCs. Conducting polymers have attracted great interest recently[14]. Some conducting polymers were prepared for application in MFCs for increasing the power density due to their high electrocatalytic activity, conductivity and chemical stability[15-17]. Carbon nanotubes were also coated on carbon cloth, carbon paper and sponge to improve the power production in MFCs because of their high specific surface area and excellent conductivity[18-20]. Besides, anode materials with porous structure allowed internal colonization, which enhanced the interaction between electrode and biofilms and consequently accelerated the electron transfer[21]. However, these materials were typically physically adsorbed on electrode surface with weak interaction which could easily be desorbed under normal experimental conditions, or they were coated on electrode surface by binders such as Nafion and polytetrafluoroethylene, which were prohibitively expensive[14, 16, 20].

As a subclass of conducting polymers, conducting polymer hydrogels have the advantageous features of both hydrogels and organic conductors and represent excellent electrochemical properties due to their intrinsic porous structure and high conductivity[22]. Conducting polymer hydrogels demonstrated excellent electrochemical activity and superior electrode performance in different electrochemical devices[23-24]. When CNTs were embedded into conducting polymer hydrogels as conductive backbones, the composite represented higher conductivity and electrochemical activity as an anode in lithium ion battery[25]. However, CNTs doped conducting polymer hydrogels without any binders for enhanced

electrocatalytic activity in MFCs have so far not been reported.

In this work, we used a facile and scalable method to synthesize conductive polypyrrole hydrogels and carbon nanotubes composite (CPHs/CNTs) directly coated on graphite felt without any binders. This composite was used as an anode in two-chambered MFCs, and its electrocatalytic activity and biocompatibility were investigated.

2. Materials and Methods

2.1. Preparation of the CPHs/CNTs

Phytic acid (an abundant natural product from plants) was used as the gelator and dopant to synthesize the CPHs/CNTs composite. The CNTs were pretreated by sonication in a 1:3 mixture of 70% nitric acid and 97% sulfuric acid for 4 h, followed by precipitation and rinsing with water[14]. Graphite felt was pretreated by immersing successively in 1 M NaOH for 12 h and then 1 M H_2SO_4 for 12 h, followed by rinsing with deionized (DI) water.

(Fig.1)

The composite was synthesized by a liquid phase reaction in a solution-based method modified from the approach as previously described[25]. The preparation mechanism and chemical structure of the polypyrrole hydrogel were illustrated in Fig.1. Specifically, the synthesis process of CPHs/CNTs was carried out via the following steps. First, 0.084 mL pyrrole monomer (98%, Sigma Aldrich) and 0.184 mL phytic acid solution (50%, wt% in water, Sigma Aldrich) was mixed with 2 mL isopropanol alcohol, taken as solution A. Solution B was prepared by dissolving 0.274 g ammonium persulfate (98%, Sigma Aldrich) into 2 mL DI water with 5 mg

dispersed CNTs. Then, these two solutions were thoroughly mixed and sonicated for 5 min to form a CPHs/CNTs liquid product. Finally, the CPHs/CNTs liquid product was coated onto graphite felt to obtain the CPHs/CNTs anode. The anode was dried in a vacuum oven and then immersed in DI water and isopropanol alcohol for 12 h to thoroughly remove excess phytic acid and inorganics salts from this anode surface.

2.2. Characterization of the CPHs/CNTs

When the CPHs/CNTs anode was dried in air, its morphology was examined by a field emission scanning electron microscopy (FESEM) (JSM-6701F, JEOL). Fourier transform infrared spectroscopy (FT-IR) was used to confirm the chemical structure of the CPHs/CNTs.

The electrochemical properties of CPHs/CNTs anode was analyzed by cyclic voltammetry (CV) in a conventional three-electrode system (CHI660D, Chenhua Instrument Co., China). The CPHs/CNTs anode served as the working electrode, whereas a Pt foil electrode was used as the counter electrode and a saturated calomel electrode (SCE) was used as the reference electrode. The CV test was performed in 0.5 mM $K_3[Fe(CN)_6]$ with 0.2 M KCl in MilliQ water, at a scanning rate of 50 mV/s and in the range of -0.2 V to 0.7 V (vs. SCE) at room temperature.

Electrochemical impedance spectroscopy (EIS) measurements were conducted over a frequency range of 0.1 Hz to 100 kHz at the working potential with a perturbation signal of 10 mV when the MFCs were operated with an external resistance of 200 Ω. The MFC anode served as the working electrode, whereas the cathode was the counter electrode and an SCE placed in the anode chamber was used

as the reference electrode.

2.3. MFC setup and operation

Two-chambered MFCs (Fig.2) separated by Proton exchange membranes (Nafion, 117, Dupont, 4 cm×4 cm) were constructed as our previous report[26]. The membrane was sequentially boiled in H_2O_2 (30%), DI water, 0.5 M H_2SO_4, and DI water (each time for 1 h). Each chamber (4 cm×2 cm×4 cm) had a total volume of about 32 mL. CPHs/CNTs and bare graphite felt (4 cm×0.3 cm×4 cm) were respectively placed in the anode chamber while graphite felt (4 cm×0.3 cm×4 cm) coated by Pt/C was used as cathodes. Titanium wire was used to connect the anodes and cathodes.

(Fig.2)

Cathodes used for MFCs were prepared by coating Pt/C catalysts onto the graphite felt surface (0.5 mg Pt/cm^2) using 5% Nafion solutions as the binder[27]. In brief, catalysts were firstly mixed and dispersed well in the Nafion and ethanol solution by ultrasonication. Then, the dispersion was coated onto the graphite felt followed by drying at room temperature.

MFCs were inoculated using a mixed bacterial culture from another MFC which was originally started up with primary clarifier overflow from Gaobeidian Wastewater Treatment Plant in Beijing and has been running for over one year. A medium containing 10 mM Sodium acetate, 50 mM phosphate buffer solution (Na_2HPO_4, 4.09 g/L and NaH_2PO_4 H_2O, 2.93 g/L), NH_4Cl (0.31 g/L), KCl (0.13 g/L), metal salt (12.5 mL/L) and vitamin (5 mL/L) solutions was used as anolyte to feed the

MFCs[28]. The catholyte was composed of 50 mM phosphate buffer solution, NH_4Cl (0.31 g/L) and KCl (0.13 g/L).

The feeding solution had been sparged with high purity nitrogen gas for 30 min to remove the oxygen harmful for electrochemically active bacteria in MFCs. The anode chamber was maintained under anaerobic condition, while the cathode chamber was purged with sterile air (10 mL/min). MFCs were operated in a temperature-controlled incubator at 30 ℃ in a fed batch mode and the feeding solutions were refreshed when the voltage dropped below 30 mV.

Cell voltages (U) across an external resistance of 200 Ω were measured and recorded using a data acquisition system (AD8201H, Ribohua Co., Ltd). Polarization and power density curves were obtained by varying the external resistance (R) from 10 Ω to 1000 Ω. Polarization was tested when the MFCs became stable and reproducible in power production. For each test, it took about 10 min to reach a stable voltage output. Current (I) was calculated by $I = U/R$, and power density (P) was normalized to the projected area of anode surface, calculated as $P = U \times I/S$, where S was the projected area of anode surface.

Biomass on electrodes was quantified by measuring bacterial protein[29]. At the end of the test, the anodes were removed from the MFCs and the washed biomass was treated in 1 M NaOH for 10 min at 100 ℃ to solubilize the attached proteins. Then the protein was measured by Bradford protein assay at 595 nm. All the experiments were carried out in duplicate and the average values with standard deviation were obtained.

3. Results and Discussion

3.1. FT-IR and morphology characterization of the CPHs/CNTs composite

(Fig.3)

The chemical structure of the as-synthesized CPHs/CNTs was analyzed by the FT-IR spectrum (Fig. 3). The absorption peak at 1552 cm^{-1} was due to the in-ring stretching of C=C bonds in the pyrrole rings. The peaks at 1307 cm^{-1} and 1045 cm^{-1} were assigned to the C-H in-plane vibration and the peak at 1189 cm^{-1} was contributed to the C-N stretching vibration. These characteristic peaks confirmed that polypyrrole hydrogels were formed through the chemical oxidation method[23, 30].

(Fig.4)

SEM images of the as-synthesized CPHs/CNTs shown in Fig.4 demonstrated that the composite had a three-dimensional porous nanostructure with CNTs as the fortifier. The nanostructured polypyrrole hydrogels provided nanoscale and micrometer sized pores, which significantly enhanced the interface between electrochemically active microorganisms and the electrodes. The highly conductive CNTs were embedded and intertwined within the hydrogel bulk, which effectively improved the electronic conductivity of the composite.

The key for the synthesis of the CPHs/CNTs composite was the phytic acid, which served as both the dopant and the gelator in the formation of the porous structure[24]. Phytic acid crosslinked the polypyrrole by protonating the nitrogens on the polypyrrole chains. Each phytic acid molecule could interact with more than one polypyrrole chains and consequently a highly crosslinked structure was formed. The

polypyrrole hydrogels were hydrophilic because there was an excess of phosphorous groups in the phytic acid, which would enhance the biofilm formation because it was demonstrated that hydrophilic surface was beneficial for the electroactive biofilm formation[31] . Therefore, the three dimensional porous structure and the hydrophilicity of this CPHs/CNTs composite was expected to exhibit excellent biocompatibility.

3.2. Electrochemical analysis of the CPHs/CNTs composite

(Fig.5)

Conductivity was a key factor for anode material in MFCs. The bare graphite felt had a high conductivity of 138 S/m, and the graphite felt coated by CPHs/CNTs had a conductivity of 130 S/m. This result indicated that CPHs/CNTs composite possessed excellent conductivity. The electron transfer property on the CPHs/CNTs surface was investigated by CV using $K_3[Fe(CN)_6]$ as a redox probe. CVs in ferrocyanide presented features of a typical quasi-reversible electron transfer process (Fig.5). The peak current of the CPHs/CNTs (3.29 ± 0.16 mA/cm^2) was almost three times as high as the peak current of the bare graphite felt (1.12 ± 0.08 mA/cm^2). The peak potential separation of the CPHs/CNTs was about 159 mV, while a much larger peak potential separation of about 278 mV was recorded for the bare graphite felt. The higher peak current and the smaller peak potential separation indicated a smaller resistance of the chemical reaction on the CPHs/CNTs surface. These results demonstrated that CPHs/CNTs significantly enhanced the electron transfer on the electrode surface.

(Fig.6)

EIS of the electrode provided key information that allowed the analysis of the electrochemical reactions on electrode surface and bacterial metabolism in MFCs. In this study, EIS experiments of the anodes were conducted to investigate the anode resistance of MFCs under working cell condition. The Nyquist plots were recorded when the steady-state current was generated (Fig.6). The plots showed semicircles over the high-frequency range followed by straight lines in the lower-frequency range. The solution resistance, resulting from the ionic resistance of electrolyte, was found at the high frequency where the plot intersected the Z' axis. The diameter of the semicircle represented the charge transfer resistance, originated from the resistance of electrochemical reactions on the electrode surface, while the straight line stood for the diffusion resistance.

The measured solution resistance and diffusion resistance of both CPHs/CNTs and bare graphite felt were very similar. However, the charger transfer resistance of the two materials was quite different. The charger transfer resistance of CPHs/CNTs was about 5.3 Ω while the value was 19.2 Ω for the bare graphite felt. The much smaller charge transfer resistance of CPHs/CNTs indicated that resistance of electrochemical reactions was reduced and extracellular electron transfer was facilitated on anode surface. This result demonstrated that CPHs/CNTs had high electrocalytic activity and greatly enhanced the microbial electron transfer in the MFC.

3.3. CPHs/CNTs anode performance in MFCs

To investigate the CPHs/CNTs composite for microbial electricity production, it

was used as an anode in a two-chambered MFC. Bare graphite felt was also studied in an MFC for control experiment. Direct anodic degradation of acetate was a form of respiration, where the terminal electron acceptor was the electrode. The oxidation of acetate availed itself of the tricarboxylic acid (TCA) cycle and membrane bound electron transfer chain. Acetate entered the TCA cycle through acetyl-CoA to generate NADH, NADPH and $FADH_2$, which were the starting points of the electron transfer chain, with electrons travelling through flavoproteins, iron-sulfur proteins, quinone pool and a series of cytochromes[32-33]. When the power generation was stable and reproducible with an external resistance of 200 Ω, a current density of about 0.16 mA /cm^2 in the MFC with the CPHs/CNTs anode and a current density of about 0.12 mA /cm^2 in the MFC with bare anode were obtained. The higher current density in this study demonstrated that CPHs/CNTs anode enhanced the current production in the MFC.

(Fig.7)

Polarization and power density curves (Fig.7) were obtained by varying the external resistance. The polarization curve indicated that CPHs/CNTs anode reduced the internal resistance of the MFC from 48 Ω to 30 Ω, which was consistent with the EIS study. MFCs with CPHs/CNTs anode had a maximum power density of 1898±46 mW/m^2, while the MFCs with bare graphite felt only exhibited a maximum power density of 871±33 mW/m^2. The considerably enhanced power density demonstrated that CPHs/CNTs material was an ideal anode to facilitate electron transfer from bacteria to electrode in MFCs.

Anode material was of great significance to the power production of MFCs because anode surface property influenced the eletroactive biofilm formation. The biomass formed on anode surface measured by protein assay indicated that the protein density on CPHs/CNTs was about 376 μg/cm^2, higher than the value of 324 μg/cm^2 on bare graphite felt. The enhanced biofilm formation was due to the CPHs/CNTs composite which exhibited three dimensional porous structures and the hydrophilicity. The porous structures allowed internal colonization to enhance the interaction between electrode and biofilm, while the hydrophilicity was conducive for electroactive biofilm attachment[21, 31]. As a result, CPHs/CNTs enhanced the biocompatibility and helped to improve the power production of MFCs.

Anode not only influenced the eletroactive biofilm formation, but also affected the extracellular electron transfer from bacteria to anode. The CPHs/CNTs represented high electrocatalytic activity in the CV and EIS study. The high electrocatalytic activity reduced the resistance of the chemical reactions on anode surface and facilitated the extracellular electron transfer. Therefore, CPHs/CNTs with high electrocatalytic activity enhanced the microbial electron transfer and contributed to higher power generation in MFCs.

The stability of the CPHs/CNTs anode was tested to investigate its application for long term operation. The CPHs/CNTs anode was removed from the MFC reactor and autoclaved after a period of three months. Then the MFC was reconstructed and operated following the procedures above. Polarization and power density curves of the reconstructed MFC were obtained when power generation was reproducible and

sustainable (Fig.7). The maximum power density of the reconstructed MFC with CPHs/CNTs anode reached 1733±46 mW/m^2, only about 8.7% decrease. This result indicated that CPHs/CNTs represented strong stability and could be used for long term operation in MFCs.

Table 1 Anode modification methods in MFCs

Modification method	MFC performance	Reference
Heat treatment of carbon mesh	Increased power density from 893 mW/m^2 to 922 mW/m^2	34
Quinone grafted on graphite felt	Increased power density from 967 mW/m^2 to 1872 mW/m^2	26
CNT/polyaniline coating on nickel foam	The power density reached 42 mW/m^2	14
Polypyrrole coated CNTs	The maximum power density was 228 mW/m^2	30
CPHs/CNTs coating on graphite felt	Enhanced power density from 871 mW/m^2 to 1898 mW/m^2	This study

Anode modification was an efficient method to enhance the performance of MFCs. Table 1 summarized some modification methods used in MFC studies. Heat treatment improved the electrochemically active surface area. However, the power density only increased by 3%[34]. Quinone covalently grafted on anode surface enhanced the electron transfer and consequently the power density, but the operation was complex and the quinine was expensive[26]. CNT/polyaniline coating and polypyrrole coated CNTs required binders such as Nafion and polytetrafluoroethylene, which were prohibitively expensive[14, 30].

CPHs/CNTs composite met the requirements of an ideal anode for MFCs: high elerocatalyic activity, excellent biocompatibility, strong chemical stability and high conductivity. Besides, the synthesis method was simple and scalable. More importantly, CPHs/CNTs composite had strong adhesion on carbon materials without

the addition of any binders. Because of these advantages, CPHs/CNTs composite held a promising potential for application in MFCs to enhance power generation.

4. Conclusion

A facile and scalable approach was used to synthesize conductive polypyrrole hydrogels/carbon nanotubes (CPHs/CNTs) that synergized the advantageous features of hydrogels and organic conductor. CV and EIS study demonstrated that this material exhibited high electrocatalytic activity, which accelerated the extracellular electron transfer on anode surface. The porous structure and hydrophilicity of CPHs/CNTs enhanced biofilm formation on anode surface. CPHs/CNTs anode increased the maximum power density greatly and exhibited high stability in a two-chambered MFC. These results demonstrated that the synthesis of the CPHs/CNTs composite provided an effective approach to enhance the power production in MFCs.

Acknowledgements

This work was supported by a grant from the Environment & Water and Industry Development Council, Singapore (MEWR 651/06/159) and a grant from the Bill & Melinda Gates Foundation (OPP109475). We also acknowledge the financial support from the National Natural Science Foundation of China (No. 21176242 & No. 21176026). Tang Xinhua thanks NUS Graduate School for Integrative Sciences and Engineering for a research scholarship support.

References

1. K. Rabaey, G. Lissens, S. D. Siciliano and W. Verstraete, *Biotechnol Lett*, 2003, **25**, 1531-1535.
2. H. Liu, R. Ramnarayanan and B. E. Logan, *Environ Sci Technol*, 2004, **38**, 2281-2285.
3. Z. W. Du, H. R. Li and T. Y. Gu, *Biotechnol Adv*, 2007, **25**, 464-482.
4. V. B. Oliveira, M. Simoes, L. F. Melo and A. M. F. R. Pinto, *Biochem Eng J*, 2013, **73**, 53-64.
5. Y. L. Huang, Z. He, J. J. Kan, A. K. Manohar, K. H. Nealson and F. Mansfeld, *Bioresource Technol*, 2012, **114**, 308-313.
6. I. S. Chang, H. Moon, J. K. Jang and B. H. Kim, *Biosens Bioelectron*, 2005, **20**, 1856-1859.
7. R. A. Rozendal, E. Leone, J. Keller and K. Rabaey, *Electrochem Commun*, 2009, **11**, 1752-1755.
8. K. B. Gregory and D. R. Lovley, *Environ Sci Technol*, 2005, **39**, 8943-8947.
9. F. Zhang, Z. Ge, J. Grimaud, J. Hurst and Z. He, *Environ Sci Technol*, 2013, **47**, 4941-4948.
10. S. E. Oh and B. E. Logan, *Water Res*, 2005, **39**, 4673-4682.
11. K. Rabaey, N. Boon, M. Hofte and W. Verstraete, *Environ Sci Technol*, 2005, **39**, 3401-3408.
12. S. Srikanth and S. V. Mohan, *Bioresource Technol*, 2012, **123**, 480-487.
13. M. H. Zhou, M. L. Chi, J. M. Luo, H. H. He and T. Jin, *J Power Sources*, 2011, **196**, 4427-4435.
14. Y. Qiao, C. M. Li, S. J. Bao and Q. L. Bao, *J Power Sources*, 2007, **170**, 79-84.
15. B. Lai, X. H. Tang, H. R. Li, Z. W. Du, X. W. Liu and Q. Zhang, *Biosens Bioelectron*, 2011, **28**, 373-377.
16. Y. J. Zou, J. Pisciotta and I. V. Baskakov, *Bioelectrochemistry*, 2010, **79**, 50-56.
17. Y. Qiao, S. J. Bao, C. M. Li, X. Q. Cui, Z. S. Lu and J. Guo, *Acs Nano*, 2008, **2**, 113-119.
18. J. J. Sun, H. Z. Zhao, Q. Z. Yang, J. Song and A. Xue, *Electrochim Acta*, 2010, **55**, 3041-3047.
19. X. Xie, M. Ye, L. B. Hu, N. Liu, J. R. McDonough, W. Chen, H. N. Alshareef, C. S. Criddle and Y. Cui, *Energ Environ Sci*, 2012, **5**, 5265-5270.
20. H. Y. Tsai, C. C. Wu, C. Y. Lee and E. P. Shih, *J Power Sources*, 2009, **194**, 199-205.
21. X. Xie, L. B. Hu, M. Pasta, G. F. Wells, D. S. Kong, C. S. Criddle and Y. Cui, *Nano Lett*, 2011, **11**, 291-296.
22. Y. Zhao, B. Liu, L. Pan and G. Yu, *Energ Environ Sci*, 2013, **6**, 2856-2870.
23. Y. Shi, L. Pan, B. Liu, Y. Wang, Y. Cui, Z. Bao and G. Yu, *Journal of Materials Chemistry A*, 2014, **2**, 6086-6091.
24. L. Pan, G. Yu, D. Zhai, H. R. Lee, W. Zhao, N. Liu, H. Wang, B. C. K. Tee, Y. Cui and Z. Bao, *P Natl Acad Sci USA*, 2012, **109**, 9287-9292.
25. B. Liu, P. Soares, C. Checkles, Y. Zhao and G. Yu, *Nano Lett*, 2013, **13**, 3414-3419
26. X. H. Tang, H. R. Li, Z. W. Du and H. Y. Ng, *Bioresource Technol*, 2014, **164**, 184-188.
27. S. Cheng, H. Liu and B. E. Logan, *Environ Sci Technol*, 2006, **40**, 364-369.
28. D. R. Lovley and E. J. P. Phillips, *Appl Environ Microb*, 1988, **54**, 1472-1480.
29. X. H. Tang, K. Guo, H. R. Li, Z. W. Du and J. L. Tian, *Bioresource Technol*, 2011, **102**, 3558-3560.

30. Y. J. Zou, C. L. Xiang, L. N. Yang, L. X. Sun, F. Xu and Z. Cao, *Int J Hydrogen Energ*, 2008, **33**, 4856-4862.
31. K. Guo, S. Freguia, P. G. Dennis, X. Chen, B. C. Donose, J. Keller, J. J. Gooding and K. Rabaey, *Environ Sci Technol*, 2013, **47**, 7563-7570.
32. D. R. Bond and D. R. Lovley, *Appl Environ Microb*, 2003, **69**, 1548-1555.
33. B. H. Kim, H. J. Kim, M. S. Hyun and D. H. Park, *J Microbiol Biotechn*, 1999, **9**, 127-131.
34. X. Wang, S. A. Cheng, Y. J. Feng, M. D. Merrill, T. Saito and B. E. Logan, *Environ Sci Technol*, 2009, **43**, 6870-6874.

Figure captions

Fig.1 The preparation mechanism and chemical structure of the polypyrrole hydrogel where phytic acid served as a dopant and a crosslinker.

Fig.2 Photograph of the two-chamber MFC reactor.

Fig.3 FT-IR spectrum of the CPHs/CNTs composite with peaks labeled.

Fig.4 SEM images of the CPHs/CNTs composite (a and b), bare graphite felt (c) and graphite felt coated by CPHs/CNTs, and biofilm formation on bare graphite felt (e) and graphite felt coated by CPHs/CNTs (f) after MFC operation.

Fig. 5 CVs of CPHs/CNTs and bare graphite felt in 0.5 mM $K_3[Fe(CN)_6]$ with 0.2 M KCl at a scanning rate of 50 mV/s.

Fig.6 EIS (Nyquist plots) of CPHs/CNTs anode and bare graphite felt anode at working potential with a perturbation signal of 10 mV in MFCs.

Fig.7 Polarization and power density curves of the MFCs with CPHs/CNTs anode and bare graphite felt anode.

Fig.1

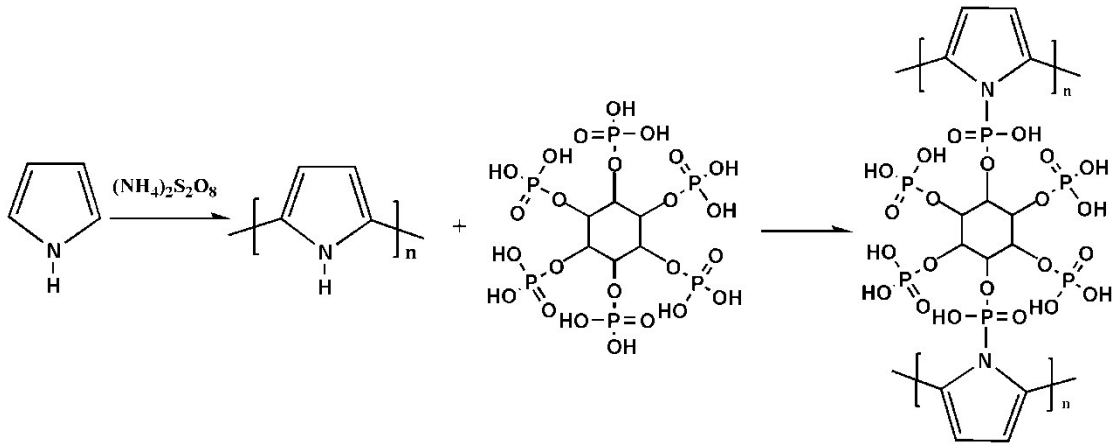

Fig.2

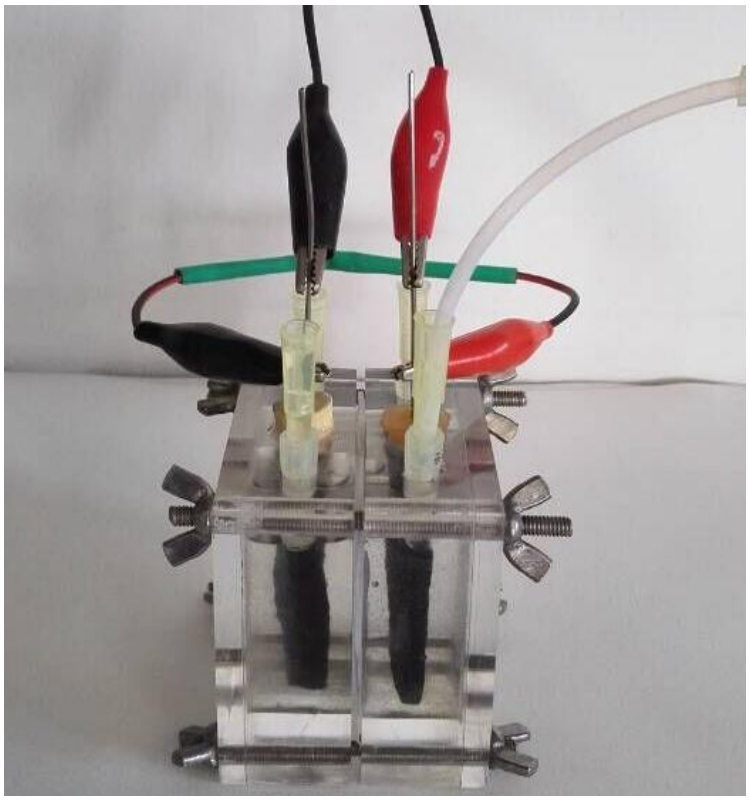

Fig.3

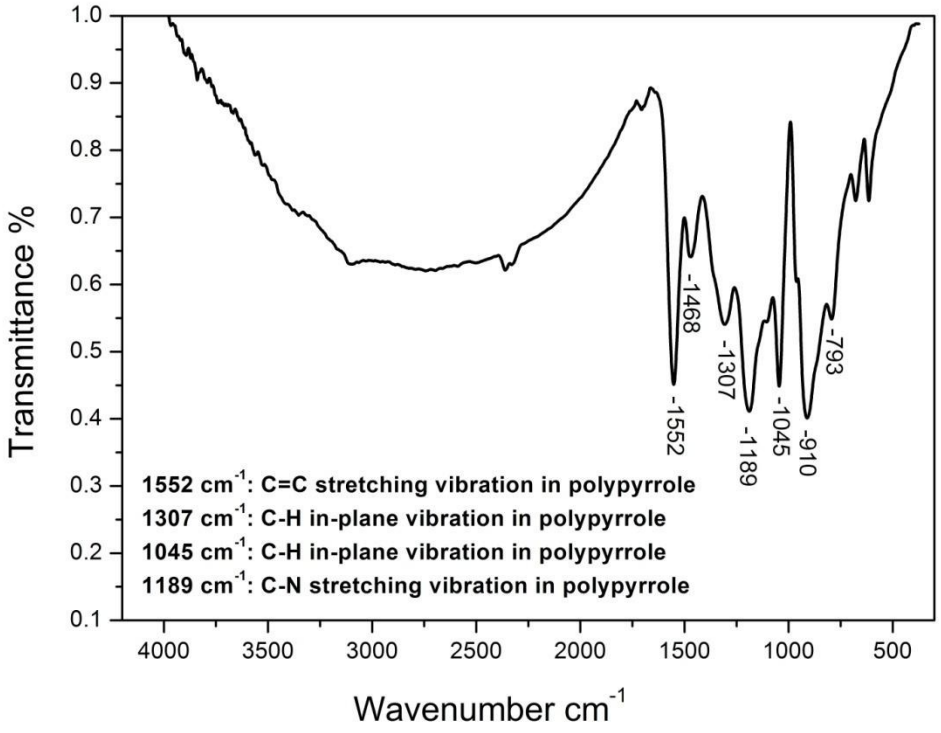

Fig.4

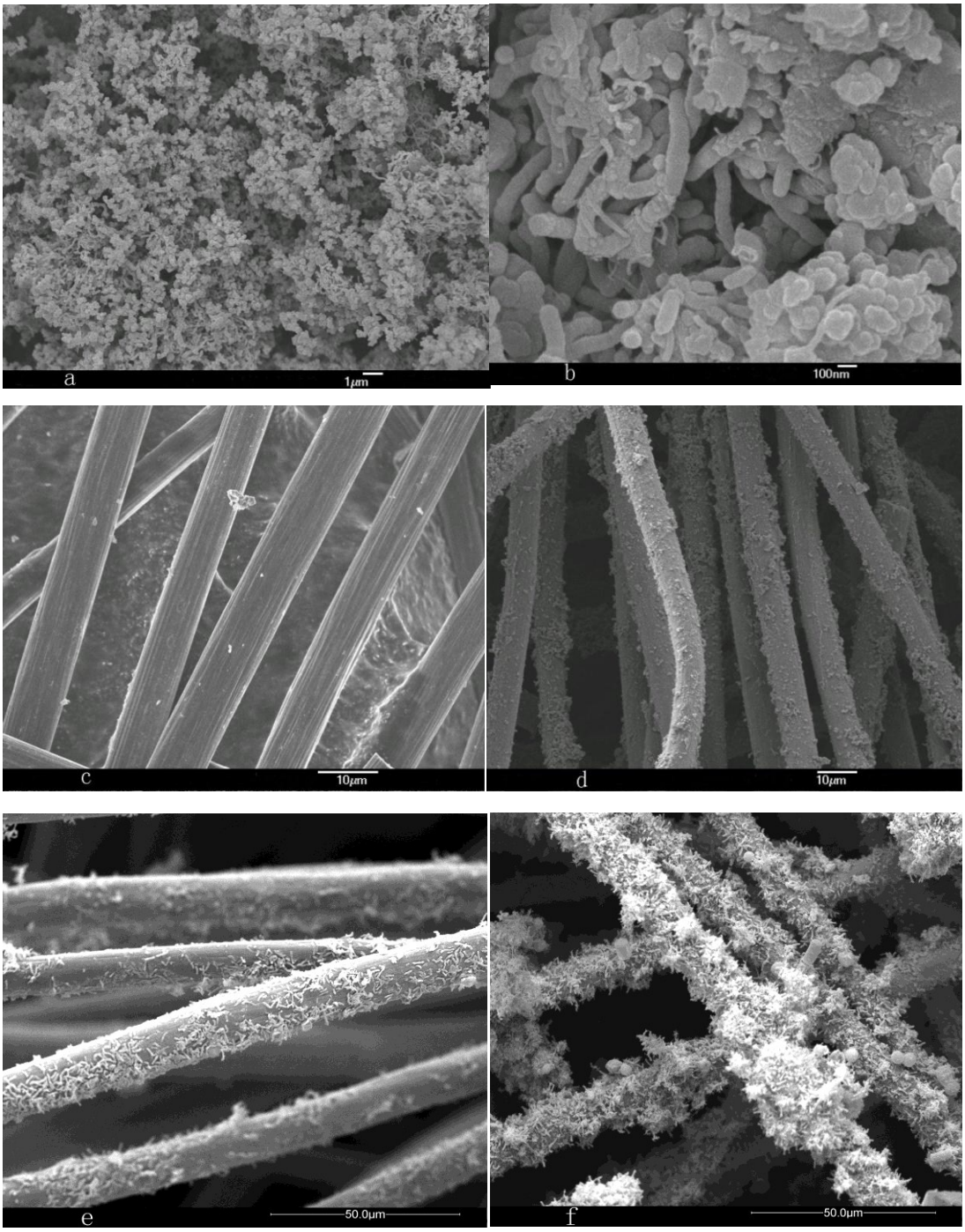

Fig.5

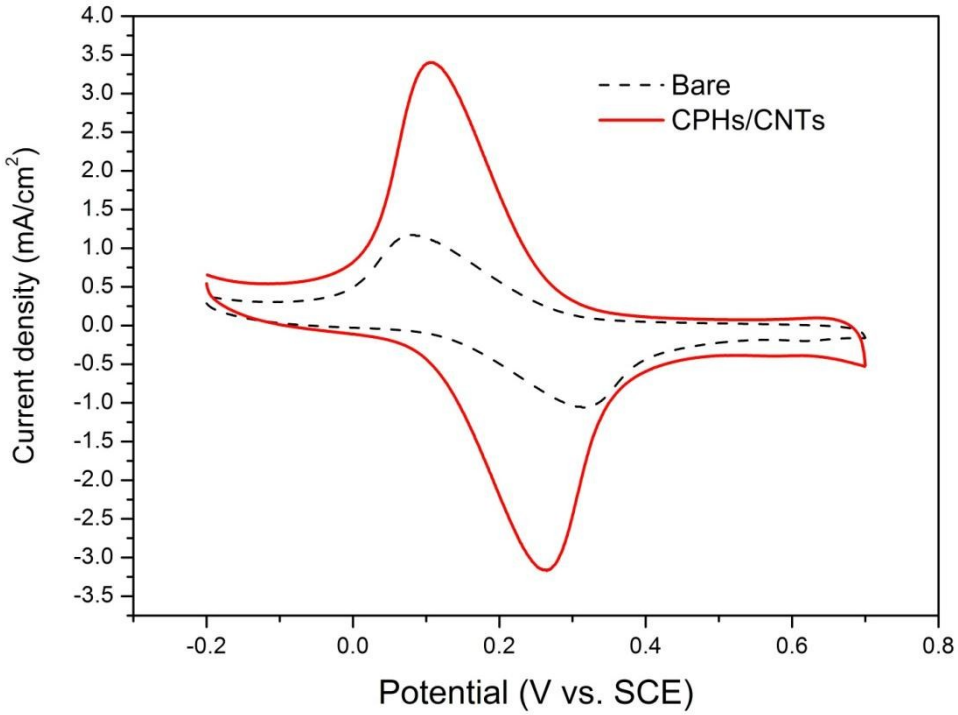

Fig.6

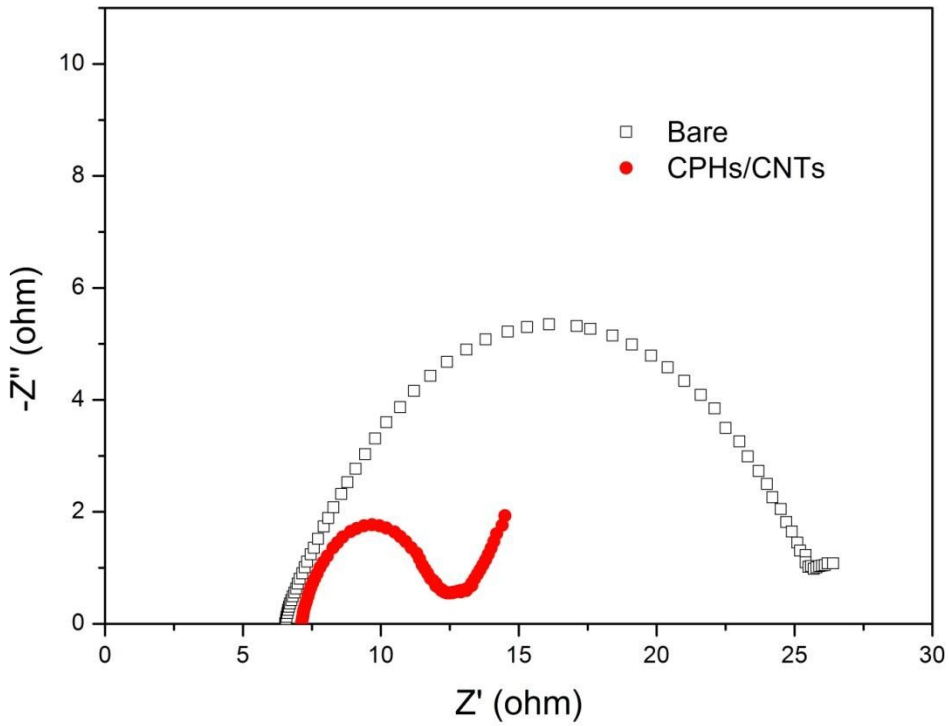

Fig. 7